Oxidatív stressz és sejthalál

Lőrincz Tamás

BME-ABÉT

doktorjelölt

Néma lombok hullása - apoptózis

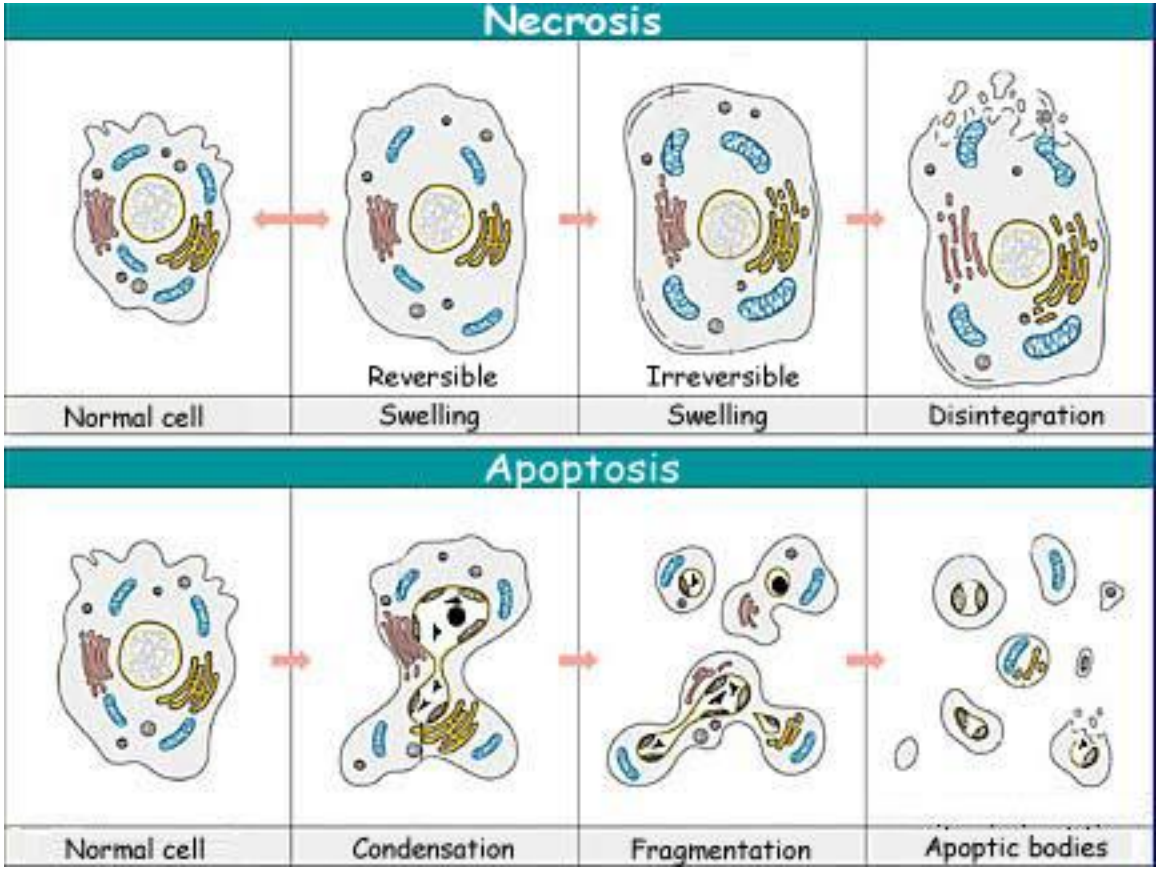

Átlagosan napi 5 – 8 x10^10 = minden 1000-ből 5

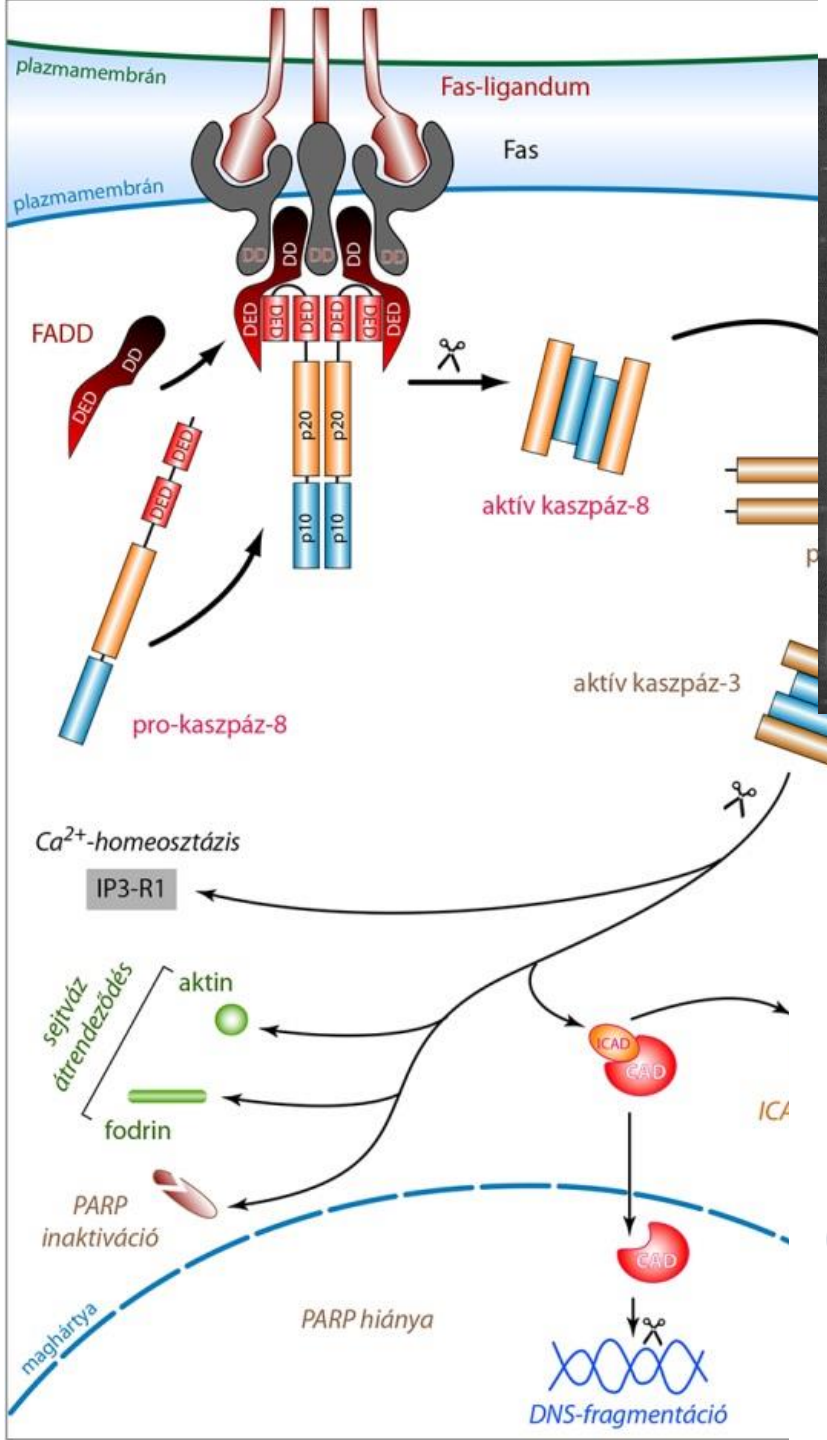
plazmamembrán
Fas-ligandum
Fas
plazmamembrán
DD
DED
FADD
p20
p10
aktív kaszpáz-8
pro-kaszpáz-8
aktív kaszpáz-3
Ca2+-homeosztázis
IP3-R1
sejtváz átrendeződés
aktin
fodrin
PARP inaktiváció
ICAD
CAD
PARP hiánya
DNS-fragmentáció
maghártya

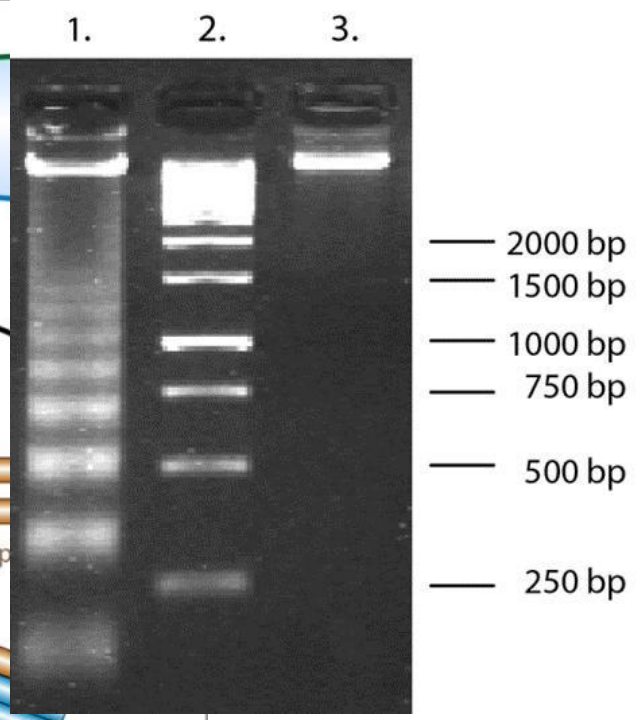
1.
2.
3.
2000 bp
1500 bp
1000 bp
750 bp
500 bp
250 bp

z-VAD-fmk

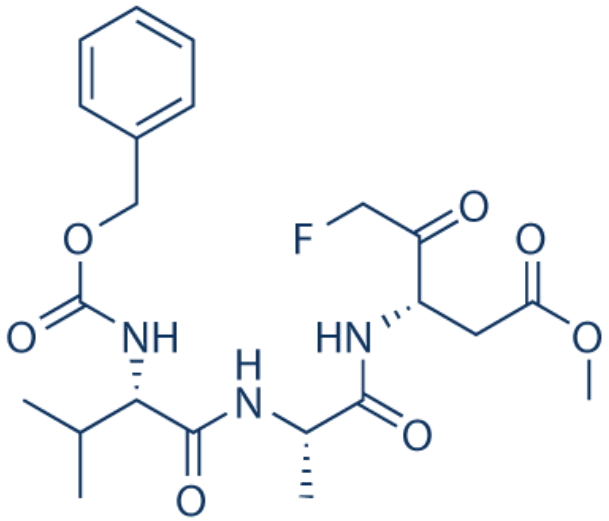
O
NH
O
H
N
HN
F
O
O
O
O

Nekroptózis

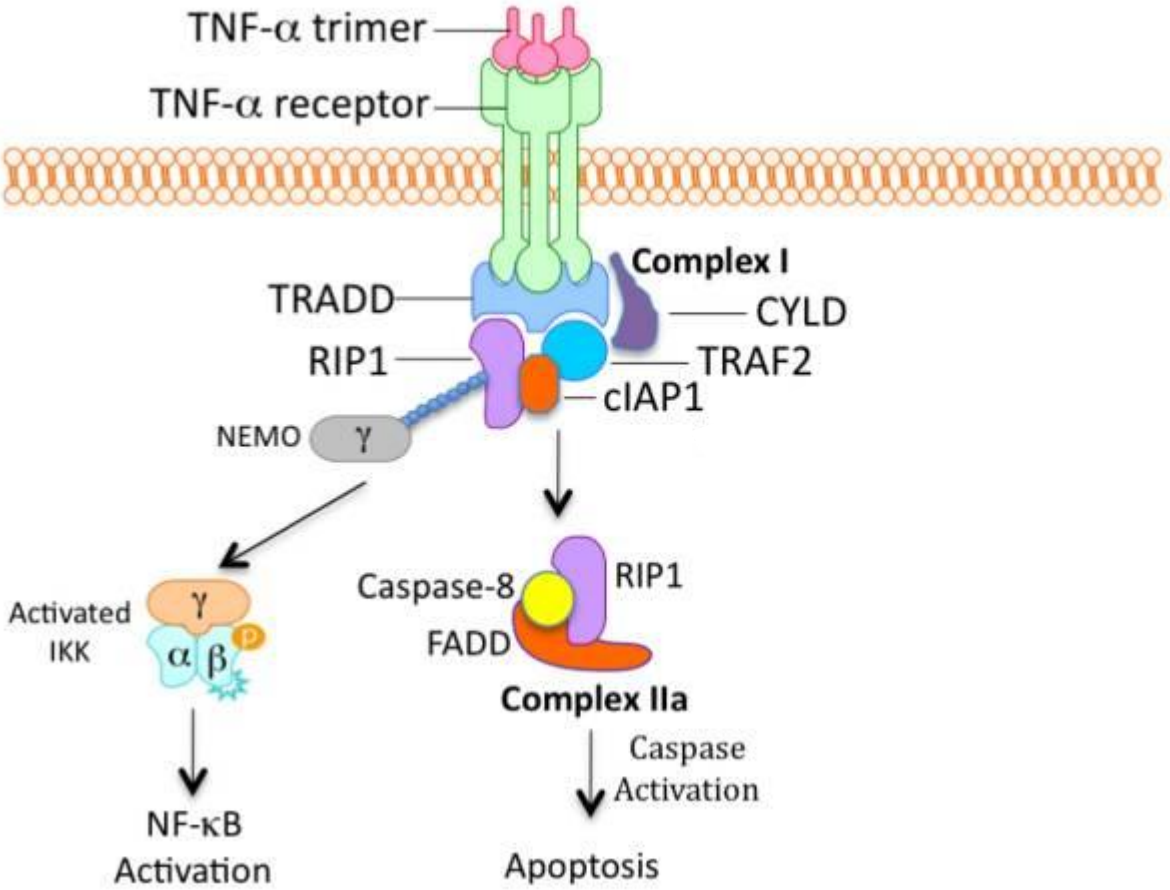

(~15 000)

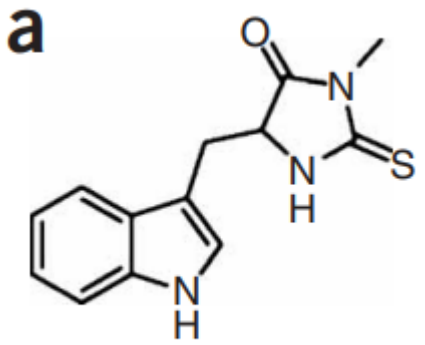

Necrostatin-1 (Nec-1, **1**)

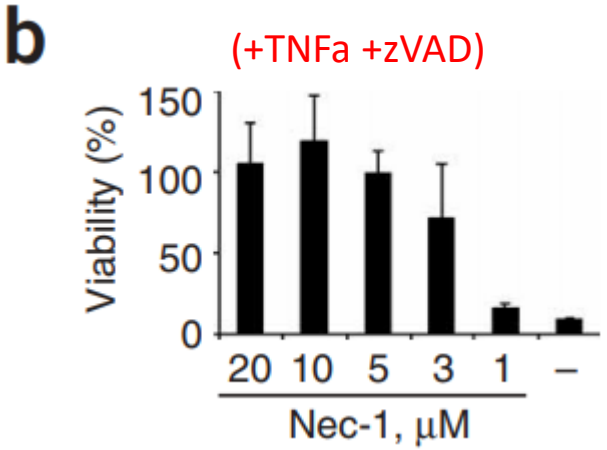

(72h, 937 cells)

Degterev A, Huang Z, Boyce M, et al (2005)
Chemical inhibitor of nonapoptotic cell death with therapeutic potential for ischemic brain injury.
Nat Chem Biol 1:112–119.

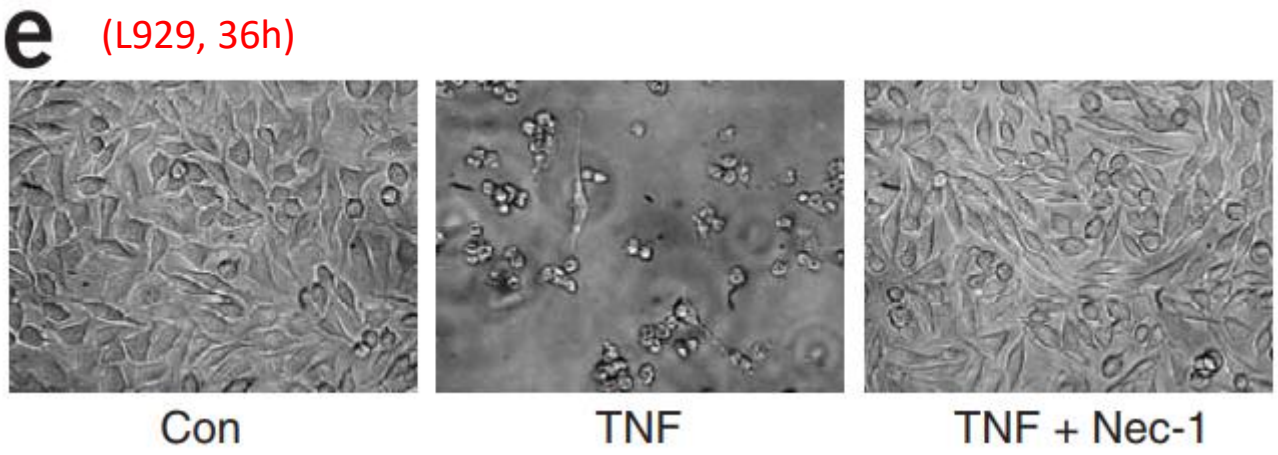

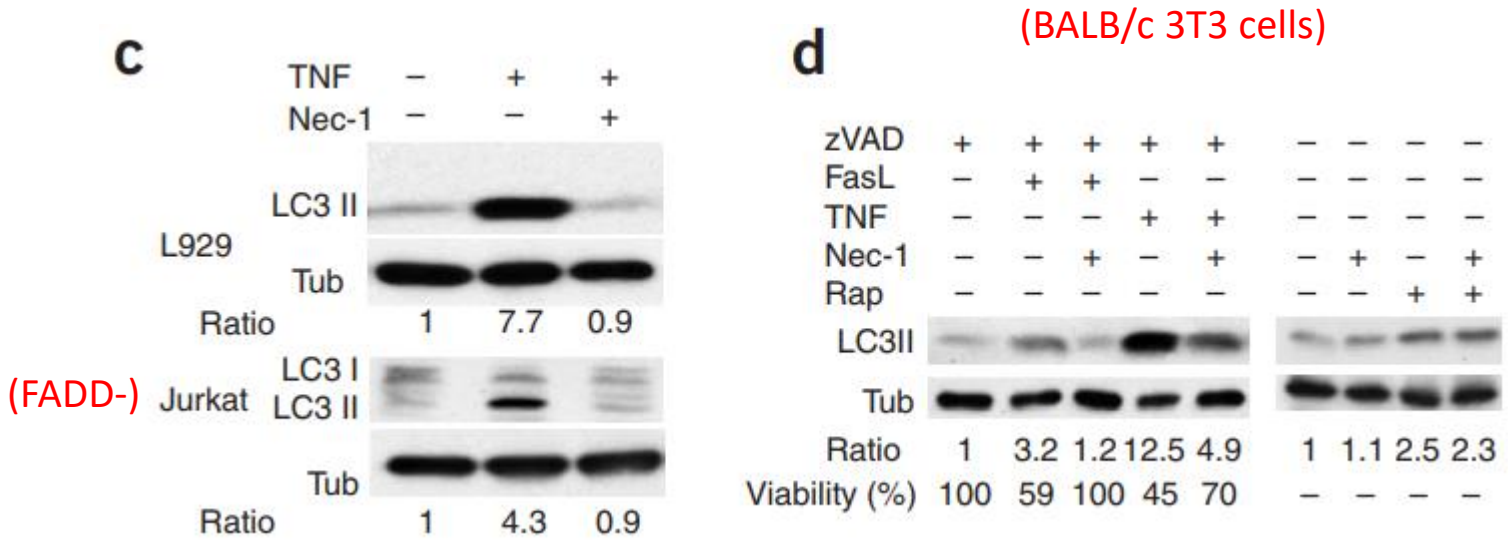

Degterev A, Huang Z, Boyce M, et al (2005)
Chemical inhibitor of nonapoptotic cell death with therapeutic potential for ischemic brain injury.
Nat Chem Biol 1:112–119.

Autofágia mechaniumusa

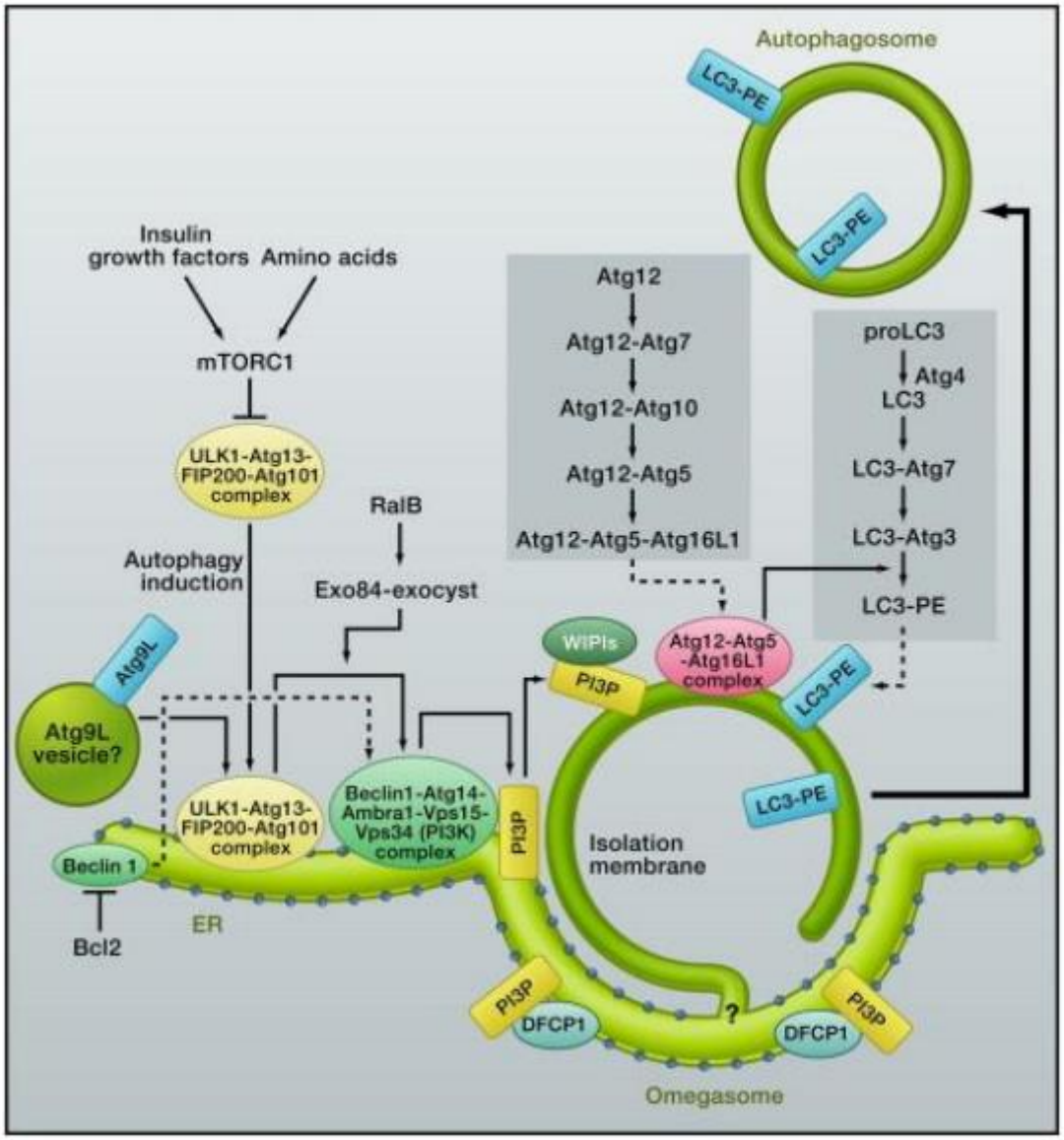

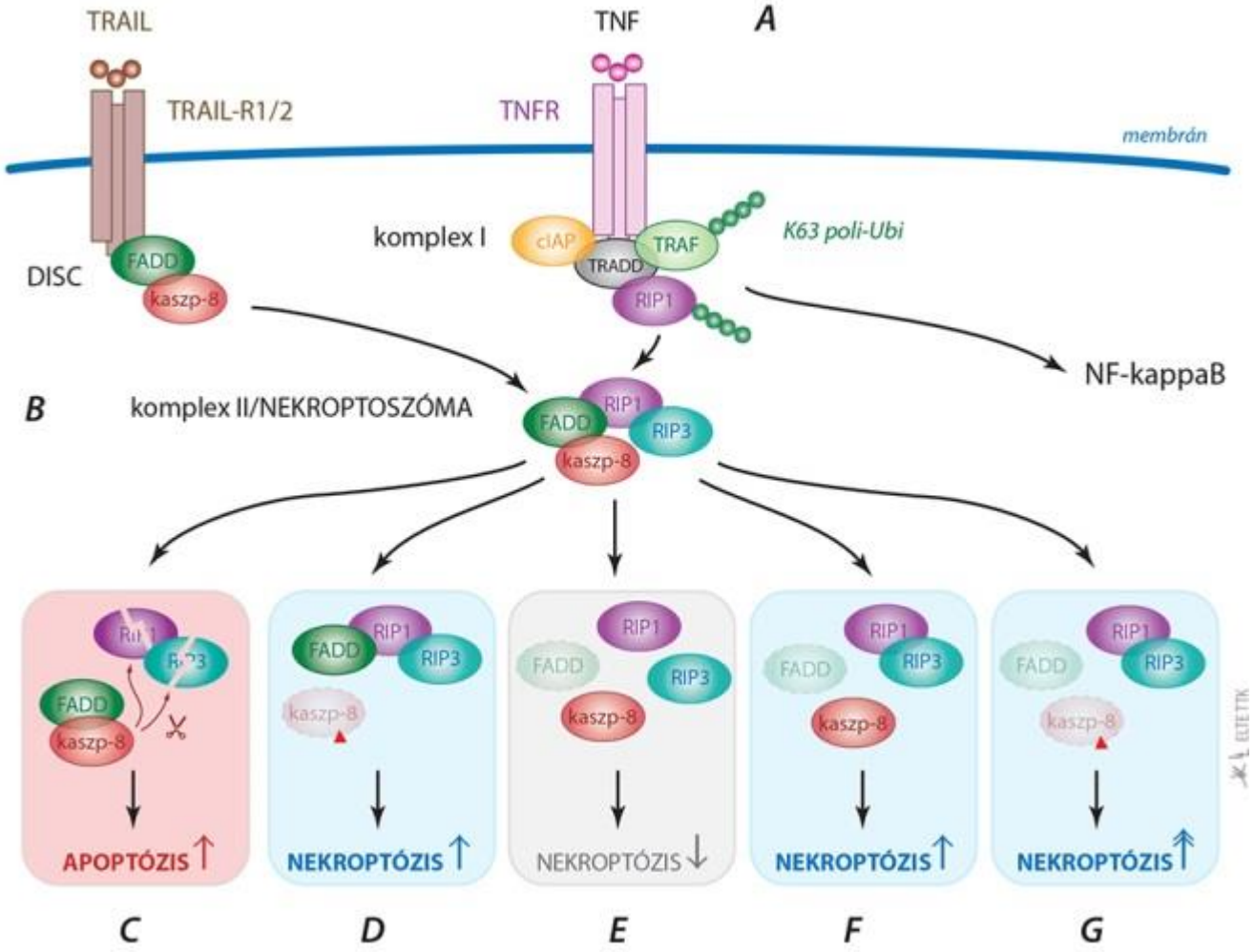

Cho YS, Challa S, Moquin D, et al (2009)
Phosphorylation-Driven Assembly of the RIP1-RIP3 Complex Regulates Programmed Necrosis and Virus-Induced Inflammation.
Cell 137:1112–1123. doi: 10.1016/j.cell.2009.05.037

Retinaleválás által kiváltott fotoreceptor nekrózis

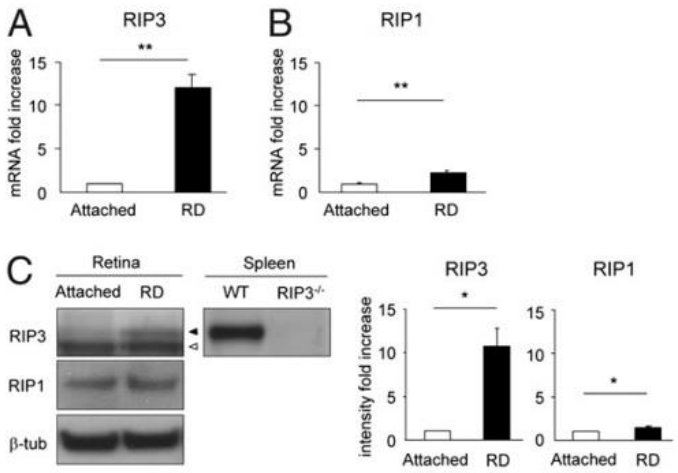

Fig. 1. Increases in RIP3 and RIP1 expression after retinal detachment. Quantitative real-time PCR analysis for RIP3 (*A*) and RIP1 (*B*) in control retina without retinal detachment and in retina 3 d after retinal detachment ($n = 9$ each); $^{**}P < 0.01$. (*C*) Western blot analysis for RIP3 and RIP1 after retinal detachment ($n = 4$ each). Lane-loading differences were normalized by levels of β-tubulin. For RIP3 analysis, spleen samples from WT and *Rip3*$^{-/-}$ animals were used as positive and negative controls, respectively. Black arrowhead indicates RIP3; white arrowhead indicates nonspecific band. The bar graphs indicate the relative level of RIP3 and RIP1 to β-tubulin by densitometric analysis, reflecting the results from four independent experiments ($^{*}P < 0.05$).

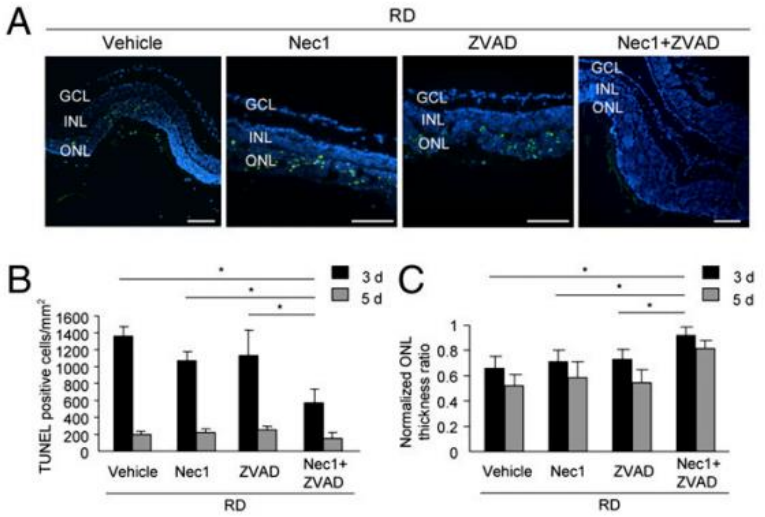

Fig. 2. Nec-1 combined with Z-VAD prevents photoreceptor loss after retinal detachment. (*A*) TUNEL (green) and DAPI (blue) staining in detached retina treated with vehicle, Nec-1, Z-VAD, or Nec-1 plus Z-VAD on day 3 after retinal detachment. Quantification of TUNEL-positive photoreceptors (*B*) and ONL thickness ratio (*C*) on day 3 (vehicle, $n = 12$; Nec-1, $n = 6$; Z-VAD, $n = 12$; Nec-1 plus Z-VAD, $n = 12$) and day 5 (vehicle, $n = 8$; Nec-1, $n = 6$; Z-VAD, $n = 8$; Nec-1 plus Z-VAD, $n = 8$) after retinal detachment ($^{*}P < 0.05$). GCL, ganglion cell layer, INL, inner nuclear layer. (Scale bar, 100 μm.)

Trichonas G, Murakami Y, Thanos A, et al (2010)
Receptor interacting protein kinases mediate retinal detachment-induced photoreceptor necrosis and compensate for inhibition of apoptosis.
Proc Natl Acad Sci 107:21695–21700

Retinaleválás által kiváltott fotoreceptor nekrózis

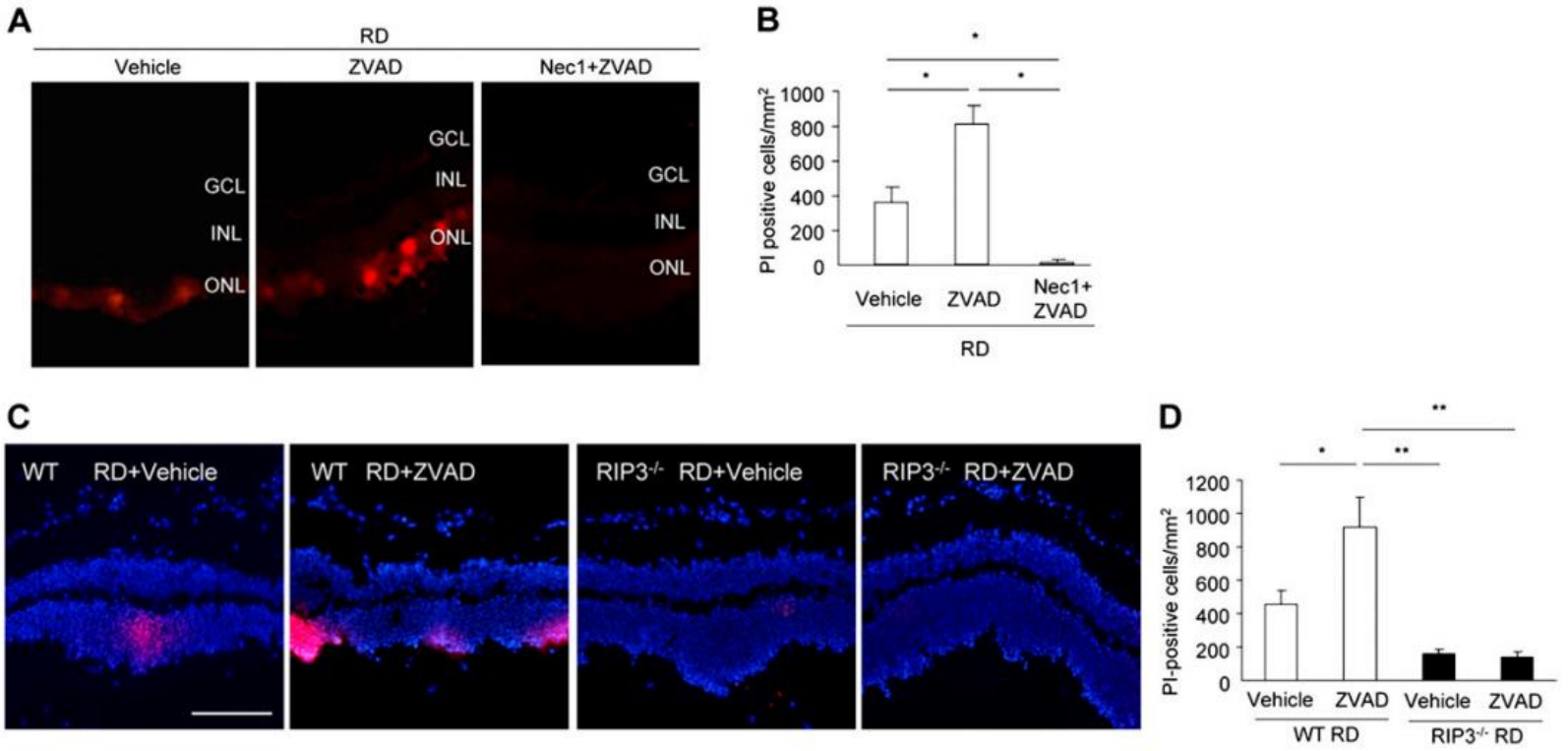

Fig. S5. PI staining (*A* and *C*) and quantification of PI-positive photoreceptors (*B* and *D*) on day 3 after retinal detachment in retina treated with vehicle, Z-VAD, or Nec-1 plus Z-VAD ($n = 6$ each; *A* and *B*) and in WT and *Rip3*$^{-/-}$ retina ($n = 5$–6; *C* and *D*); $^{*}P < 0.05$; $^{**}P < 0.01$. (Scale bar, 100 μm.)

Trichonas G, Murakami Y, Thanos A, et al (2010)
Receptor interacting protein kinases mediate retinal detachment-induced photoreceptor necrosis and compensate for inhibition of apoptosis.
Proc Natl Acad Sci 107:21695–21700

MLKL, necrosulfonamide

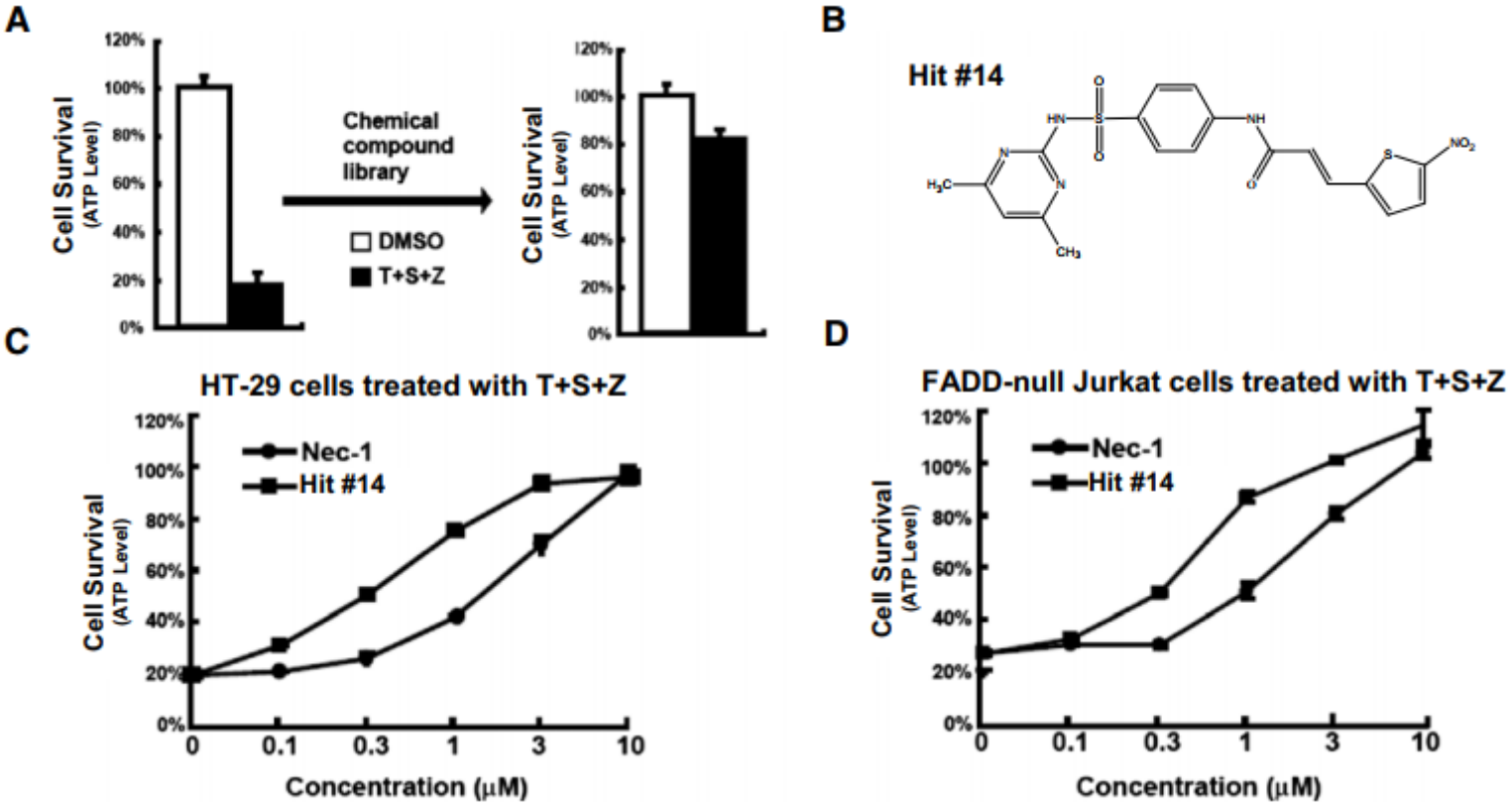

Sun L, Wang H, Wang Z, et al (2012)
Mixed lineage kinase domain-like protein mediates necrosis signaling downstream of RIP3 kinase.
Cell 148:213–227. doi: 10.1016/j.cell.2011.11.031

MLKL, necrosulfonamide

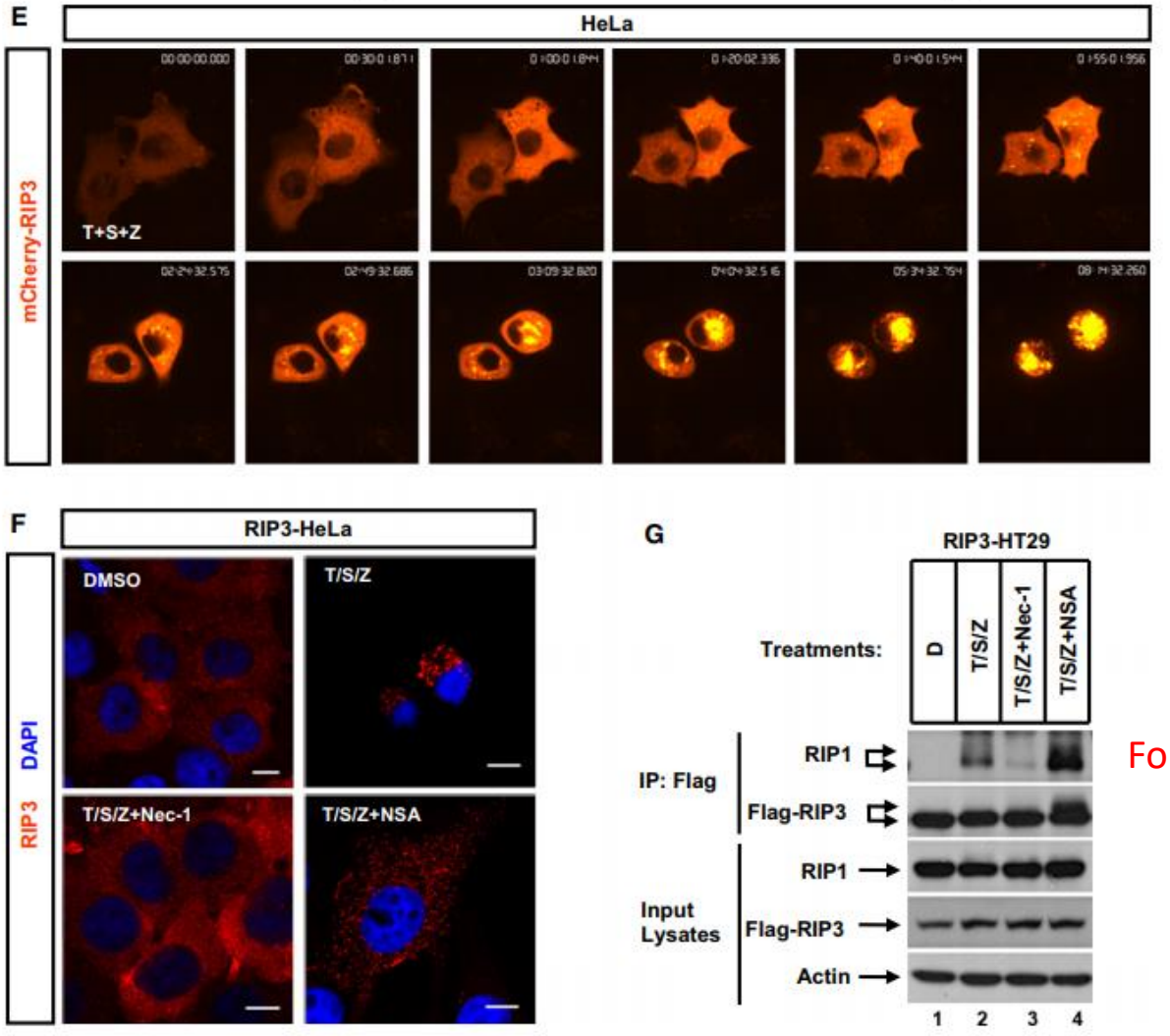

RIP3 punctae, de kisebbek mint NSA nélkül

Fokozott RIP1/3-P

Sun L, Wang H, Wang Z, et al (2012)
Mixed lineage kinase domain-like protein mediates necrosis signaling downstream of RIP3 kinase.
Cell 148:213–227. doi: 10.1016/j.cell.2011.11.031

MLKL, necrosulfonamide

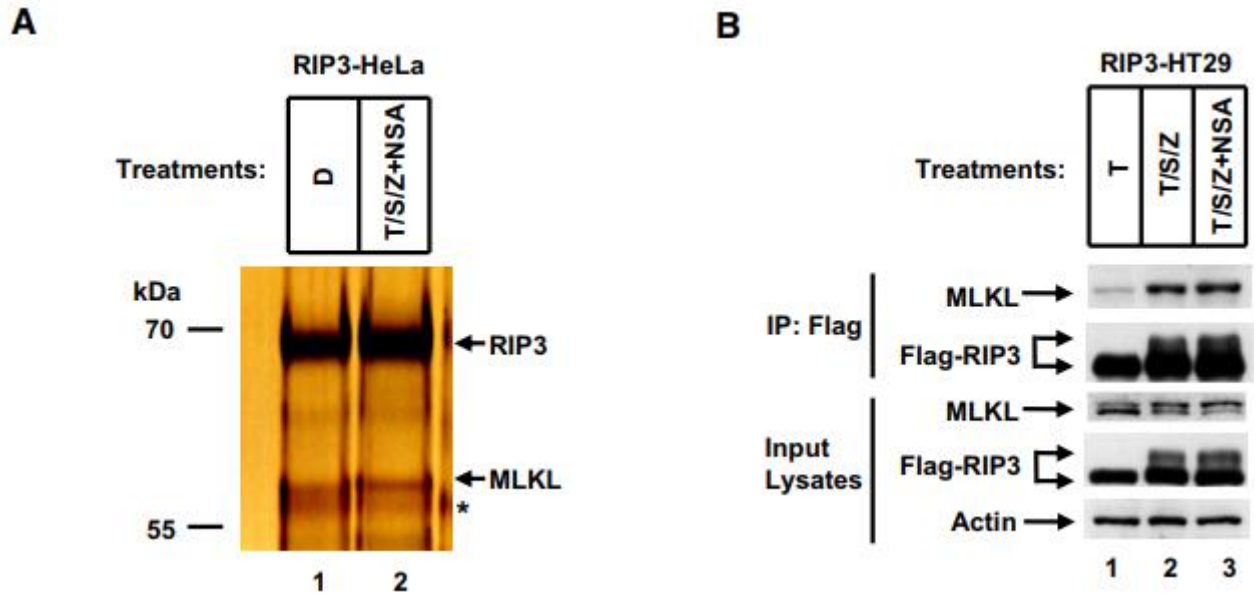

Figure 2. MLKL Is Required for TNF-α-Induced Necrosis

(A) Identification of MLKL as a necrosome component. RIP3-HeLa cells (RIP3 was double tagged with Flag and HA) were treated as indicated. The cells were then harvested, and whole-cell extracts were sequentially immunoprecipitated with anti-Flag and anti-HA antibodies as described in Experimental Procedures. The peptide-eluted RIP3-associated complexes were then analyzed by SDS-PAGE followed by silver staining. The indicated bands were excised and subjected to mass spectrometry analysis. The asterisk (*) denotes the IgG heavy chain.

(B) The MLKL-RIP3 interaction is enhanced following necrosis induction. Flag-tagged RIP3-HT-29 cells were treated with the indicated stimuli for 6 hr. The cells were then harvested, and the whole-cell extracts were immunoprecipitated with anti-Flag antibody as described in Experimental Procedures. The immunocomplexes were analyzed by western blot analysis using the indicated antibodies. Aliquots of 20 μg whole-cell lysates (Input) were subjected to SDS-PAGE followed by western blot analysis of RIP1, RIP3, and MLKL. β-Actin is shown as a loading control.

Sun L, Wang H, Wang Z, et al (2012)
Mixed lineage kinase domain-like protein mediates necrosis signaling downstream of RIP3 kinase.
Cell 148:213–227. doi: 10.1016/j.cell.2011.11.031

Genotípus-szelektív antitumor ágensek

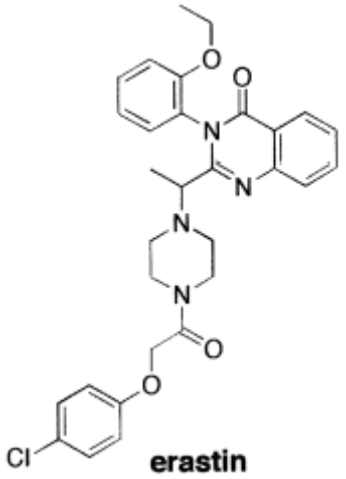

erastin

23 550 vegyület, ebből 20 000 kombinatorikus

Table 1. Potencies of tumor-selective compounds in engineered cell lines

	BJ	BJ-TERT	BJ-TERT/LT/ST	BJ-TERT/LT/ST/Ras^{v12}	BJ-TERT/LT/Ras^{v12}	BJ-TERT/LT/Ras^{v12} ST	BJ-TERT/p53DD/CDK4^{R24C}/cyclinD1/ST/Ras^{v12}	TIP5-TERT	TIP5-TERT/LT	TIP5-TERT/LT/ST	TIP5-TERT/LT/ST/Ras^{v12}	TIP-TERT/E6	TIP5-TERT/E6E7	TIP5-TERT/E6E7/ST	TIP5-TERT/E6E7/ST/Ras^{v12}	Tumor selectivity	Genetic basis of selectivity
Echinomycin	>5	0.312	0.0048	0.0012	0.0048	0.0012	0.078	>5	5	0.0048	0.0024	>5	0.048	0.048	0.0048	>8333	nonspecific
Sangivamycin	0.312	0.039	0.195	0.078	0.078	0.078	0.078	1.25	0.312	0.039	0.078	0.156	0.078	0.078	0.078	4	nonspecific
NSC146109	>5	5	2.5	2.5	5	2.5	5	>5	>5	5	2.5	5	2.5	2.5	2.5	>4	nonspecific
Bouvardin	0.312	0.078	0.0195	0.078	0.078	0.0195	0.156	>5	0.312	0.039	0.039	0.078	0.039	0.039	0.078	4	nonspecific
Mitoxantrone	5	1.25	0.312	0.312	1.25	0.312	1.25	>5	1.25	0.625	1.25	1.25	0.625	0.625	1.25	16	TERT/RB
Doxorubicin	>5	1.25	0.312	1.25	1.25	1.25	1.25	>5	1.25	0.625	0.625	5	1.25	1.25	1.25	>8	TERT/RB
Daunorubicin	5	1.25	0.312	0.312	1.25	0.625	0.625	>5	1.25	0.625	0.625	5	0.625	0.625	0.625	16	TERT/RB
Camptothecin	>5	>5	1.25	0.0195	1.25	0.0195	1.25	>5	>5	0.156	0.156	>5	0.625	0.156	0.156	>512	RAS^{v12}/PP2A/RB
Erastin	>5	>5	>5	1.25	>5	1.25	2.5	>5	>5	5	2.5	>5	>5	>5	5	>8	RAS^{v12}/PP2A

Nine tumor-selective compounds were retested in 16-point, two-fold dilution dose-curves in all engineered cell lines. The table lists the concentration (in μg/ml) required to achieve 50% inhibition of calcein AM staining (IC_{50}) for each compound in each cell line. The IC_{50} in primary BJ cells was divided by the IC_{50} in BJ-TERT/LT/ST/RAS^{V12} tumorigenic cells to obtain a tumor selectivity ratio for each compound. The compound selectivity for each genetic element was determined by calculating the selectivity ratio for each subsequent pair of cell lines in a series. Small T oncoprotein-selective compounds were considered to be selective for PP2A (the target of small T oncoprotein), whereas E6-selective compounds were considered to be selective for loss of p53, and E7-selective compounds were considered to be selective for loss of RB.

Dolma S, Lessnick SL, Hahn WC, Stockwell BR (2003)
Identification of genotype-selective antitumor agents using synthetic lethal chemical screening in engineered human tumor cells.
Cancer Cell 3:285–296.

Genotípus-szelektív antitumor ágensek

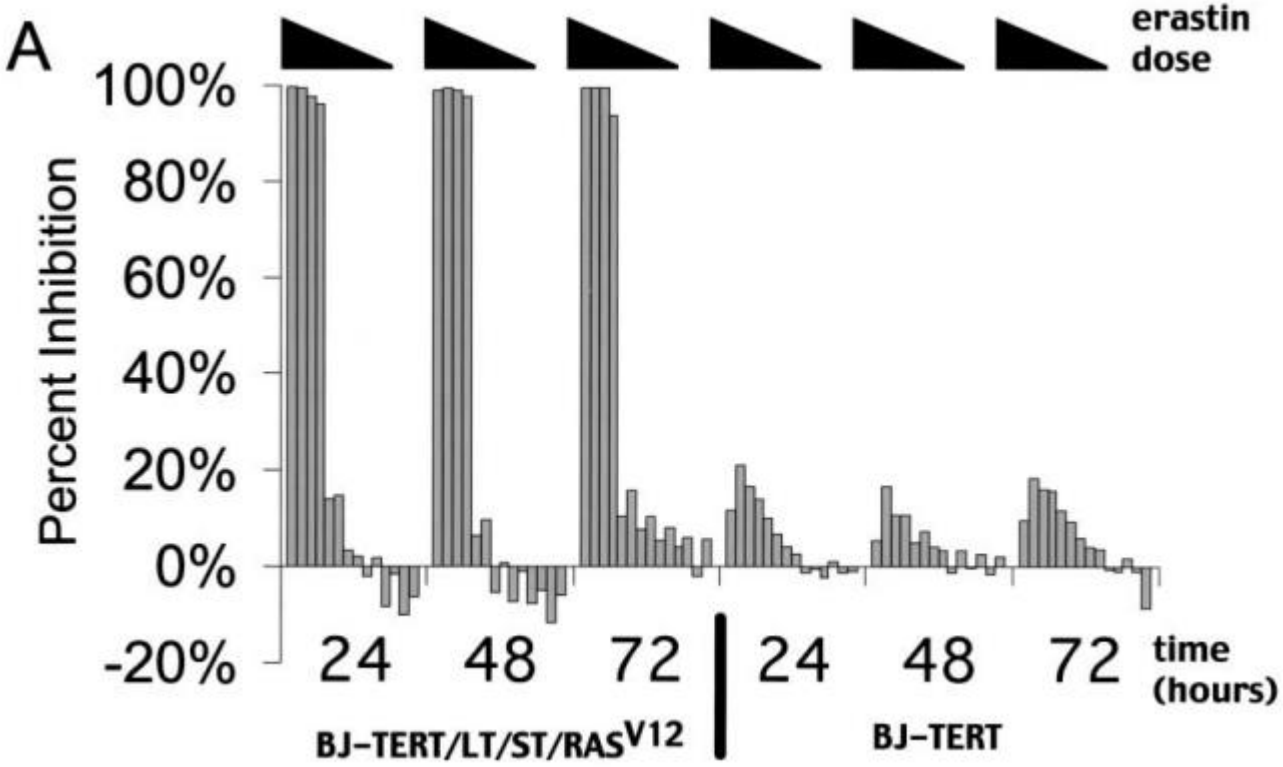

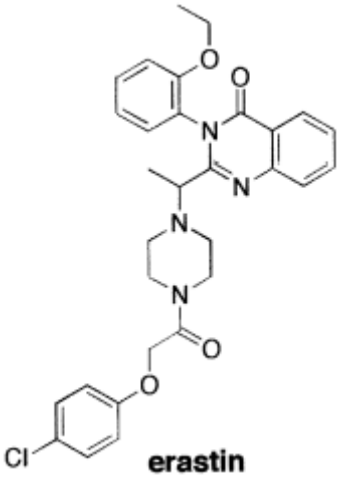

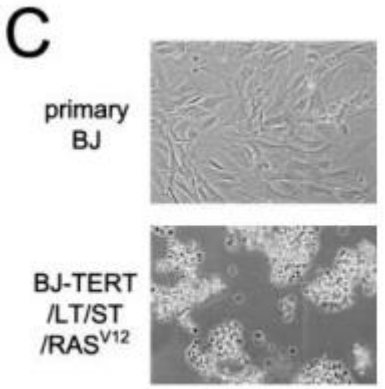

Dolma S, Lessnick SL, Hahn WC, Stockwell BR (2003)
Identification of genotype-selective antitumor agents using synthetic lethal chemical screening in engineered human tumor cells.
Cancer Cell 3:285–296.

Genotípus-szelektív antitumor ágensek

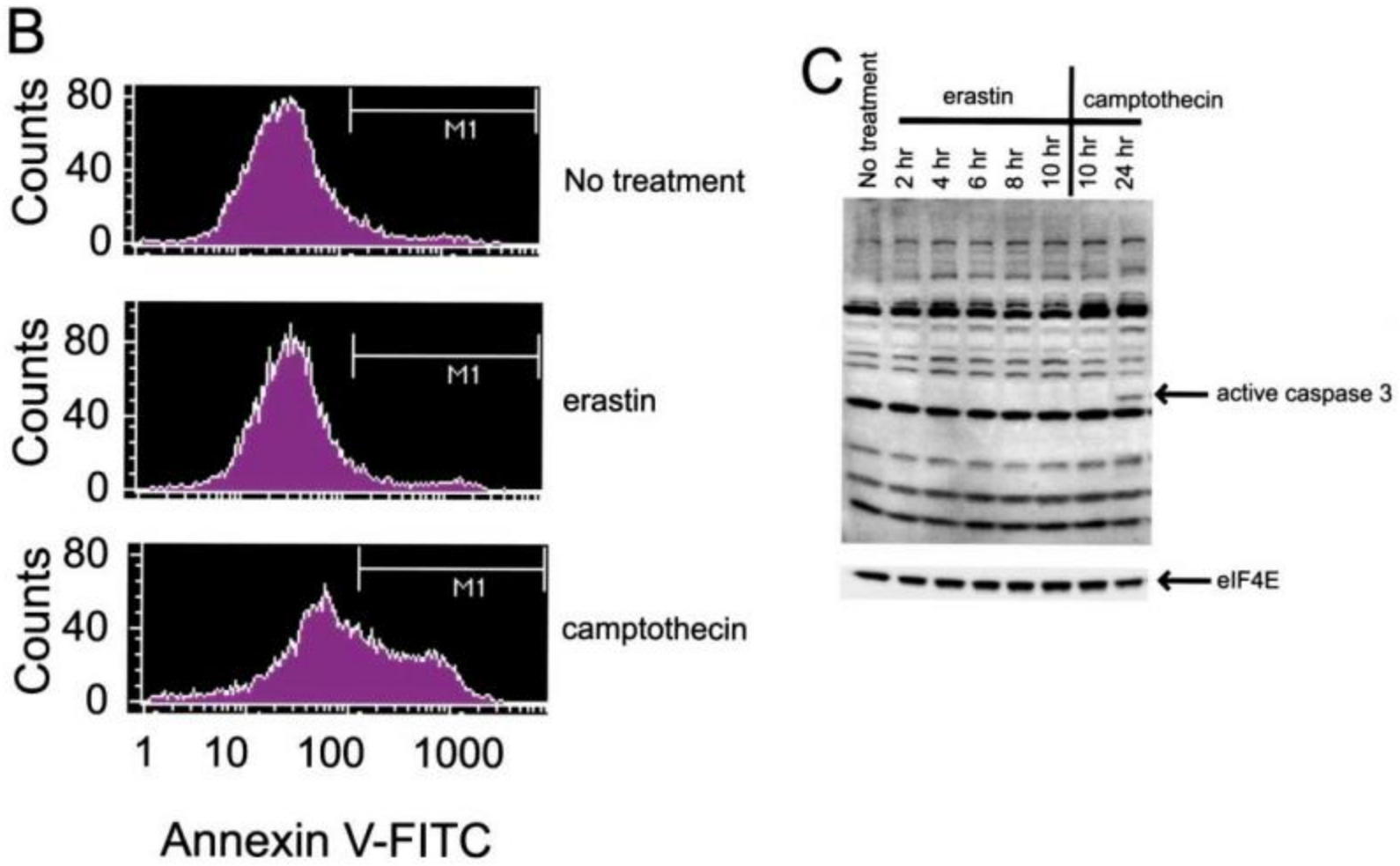

Dolma S, Lessnick SL, Hahn WC, Stockwell BR (2003)
Identification of genotype-selective antitumor agents using synthetic lethal chemical screening in engineered human tumor cells.
Cancer Cell 3:285–296.

Genotípus-szelektív antitumor ágensek

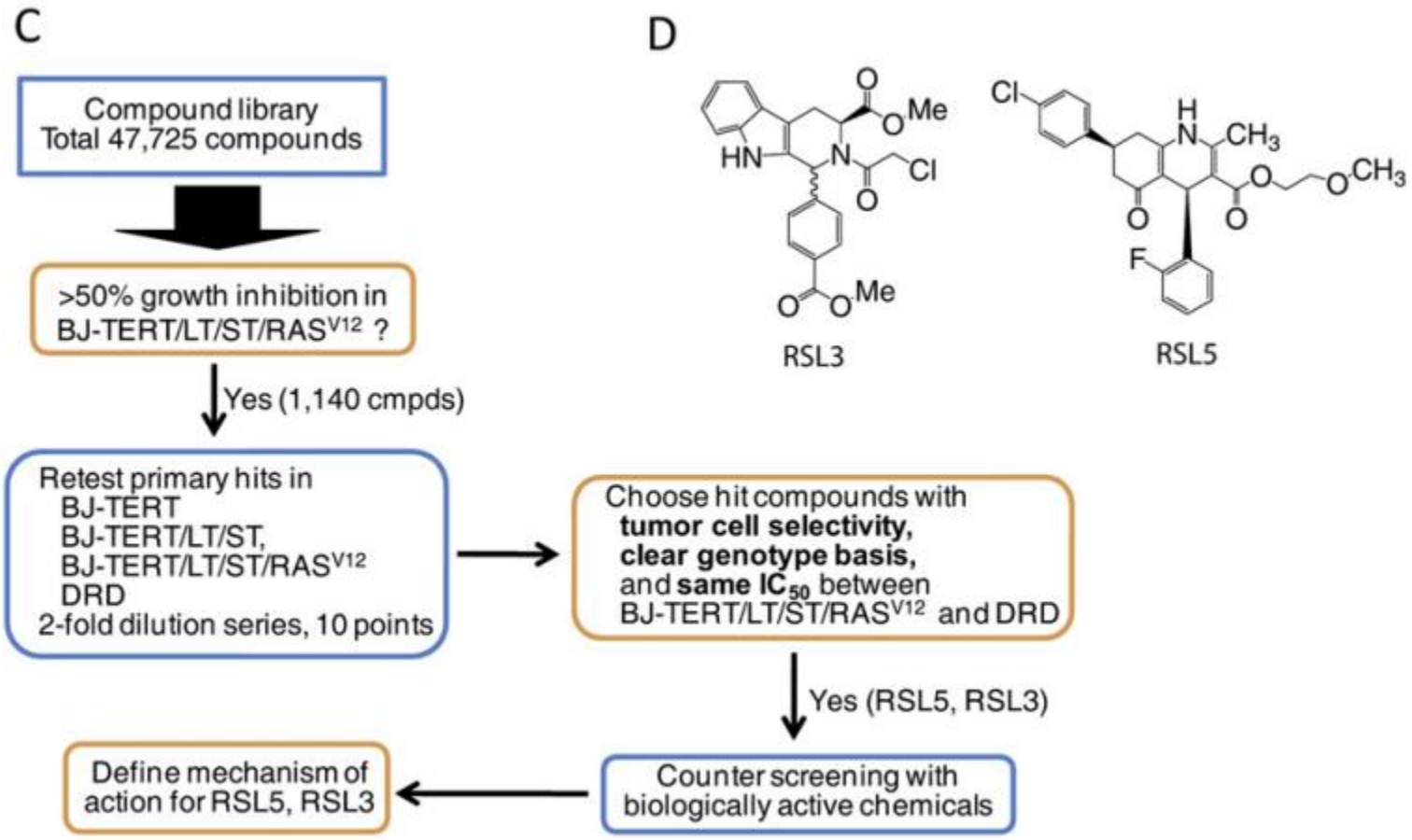

Yang WS, Stockwell BR (2008)
Synthetic Lethal Screening Identifies Compounds Activating Iron-Dependent, Nonapoptotic Cell Death in Oncogenic-RAS-Harboring
Cancer Cells. Chem Biol 15:234–245.

Genotípus-szelektív antitumor ágensek

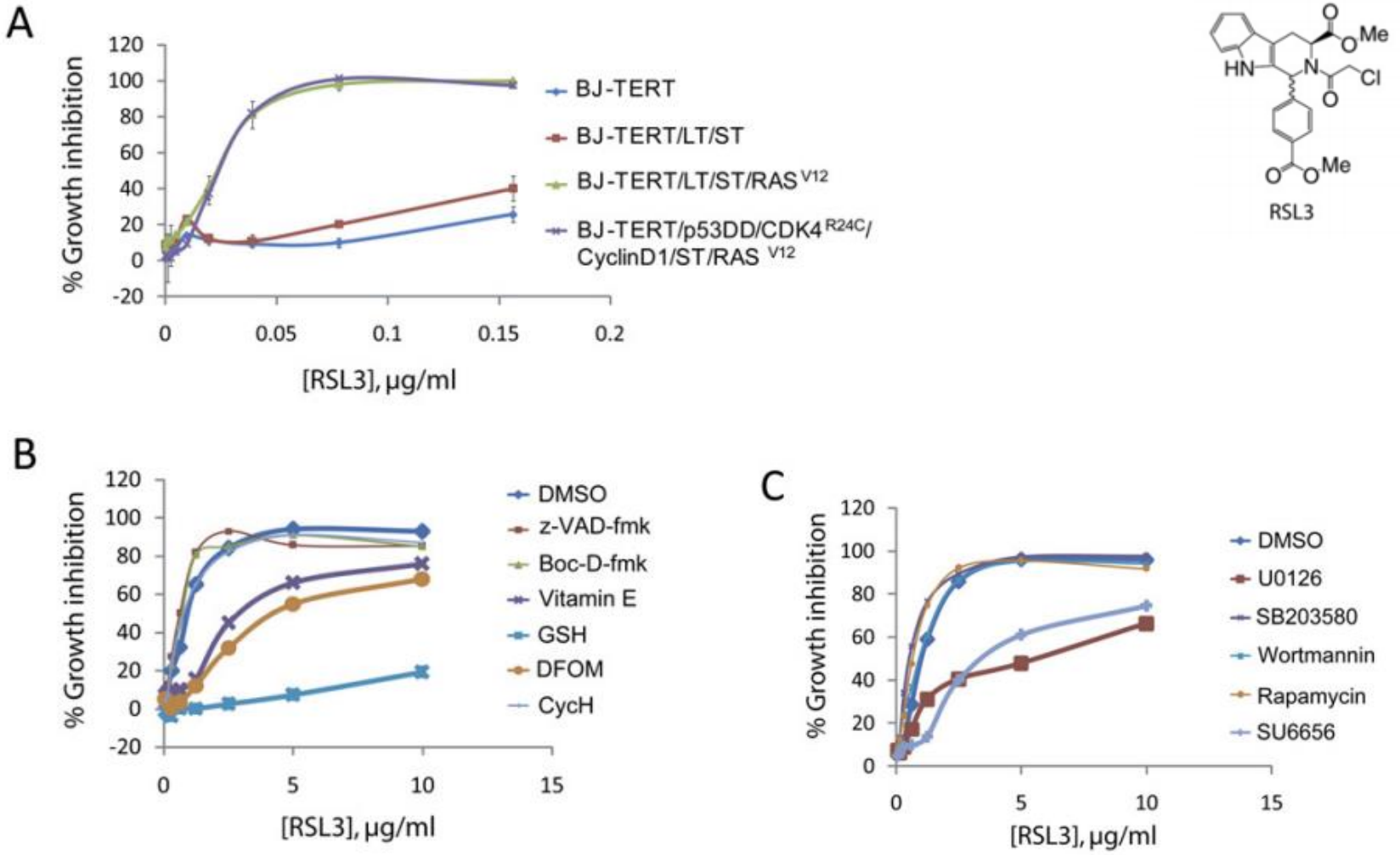

Yang WS, Stockwell BR (2008)
Synthetic Lethal Screening Identifies Compounds Activating Iron-Dependent, Nonapoptotic Cell Death in Oncogenic-RAS-Harboring
Cancer Cells. Chem Biol 15:234–245.

Ferroptózis

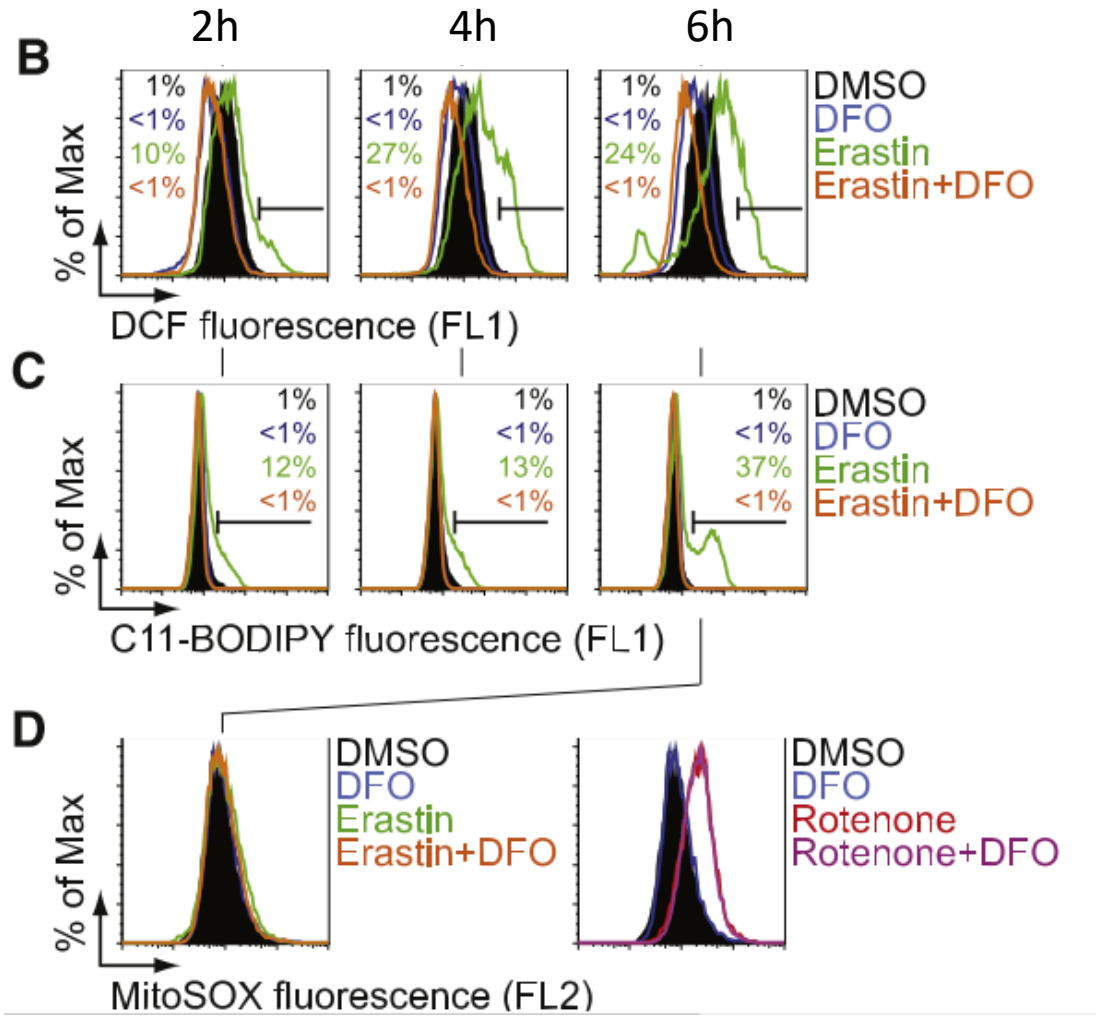

Dixon SJ, Lemberg KM, Lamprecht MR, et al (2012)
Ferroptosis: An iron-dependent form of nonapoptotic cell death.
Cell 149:1060–1072. doi: 10.1016/j.cell.2012.03.042

Oxidatív stressz

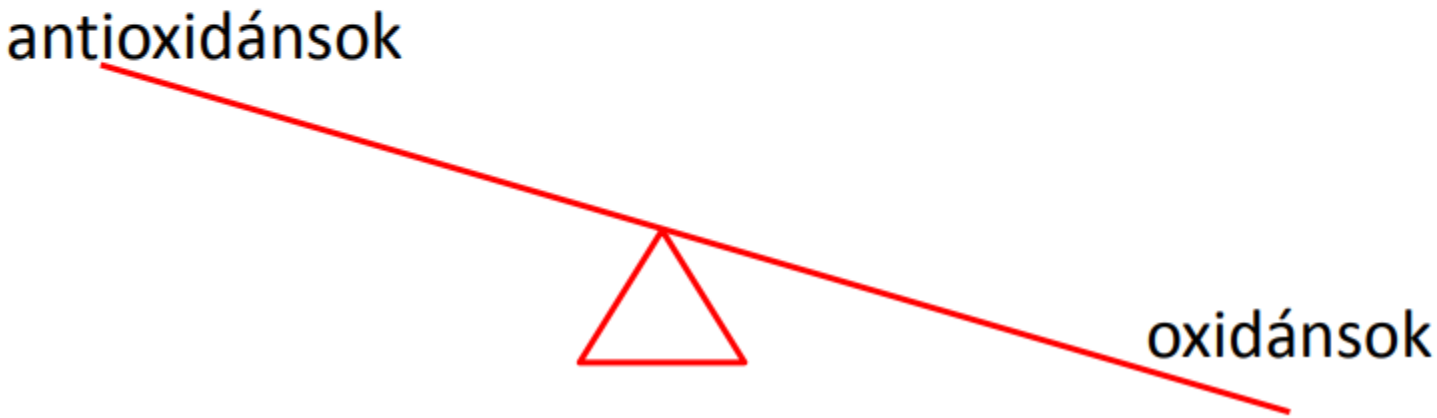

Ferroptózis

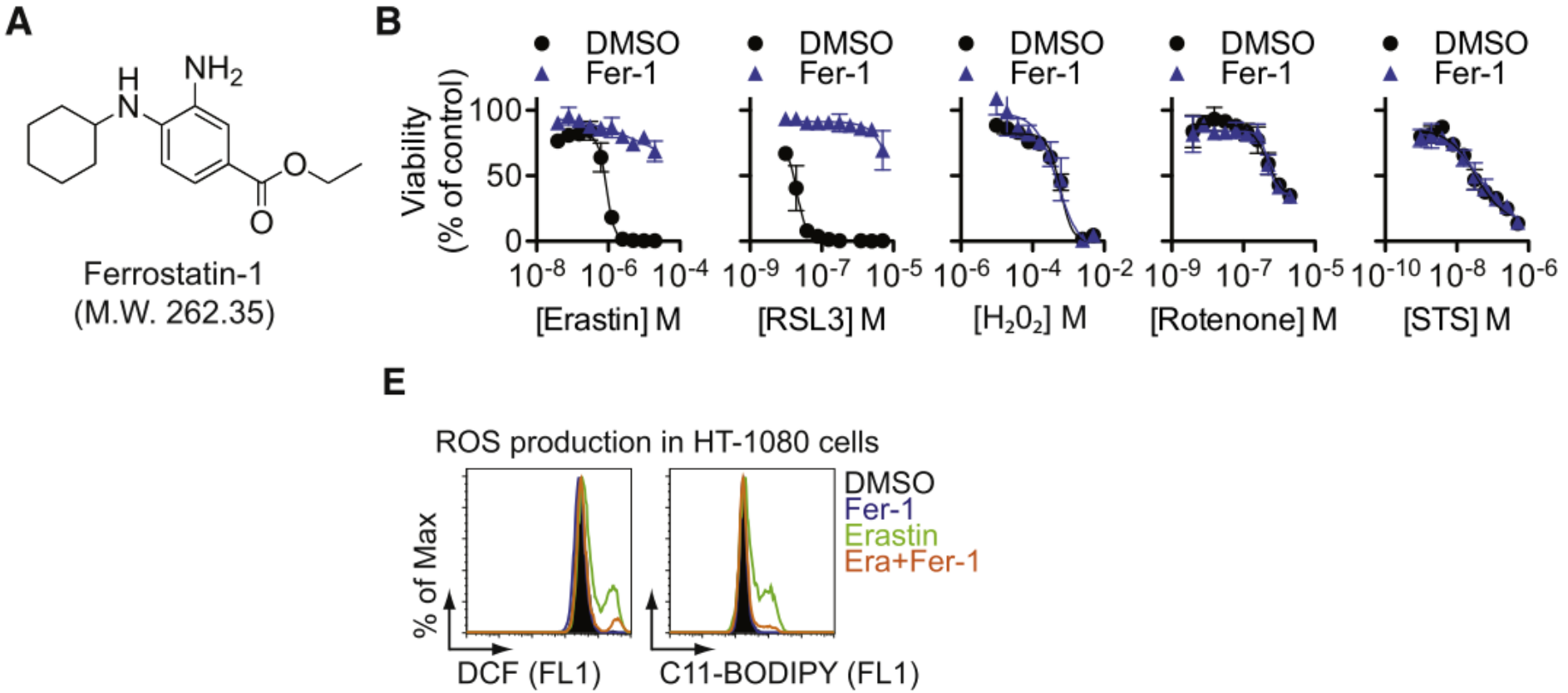

Dixon SJ, Lemberg KM, Lamprecht MR, et al (2012)
Ferroptosis: An iron-dependent form of nonapoptotic cell death.
Cell 149:1060–1072. doi: 10.1016/j.cell.2012.03.042

Ferroptózis

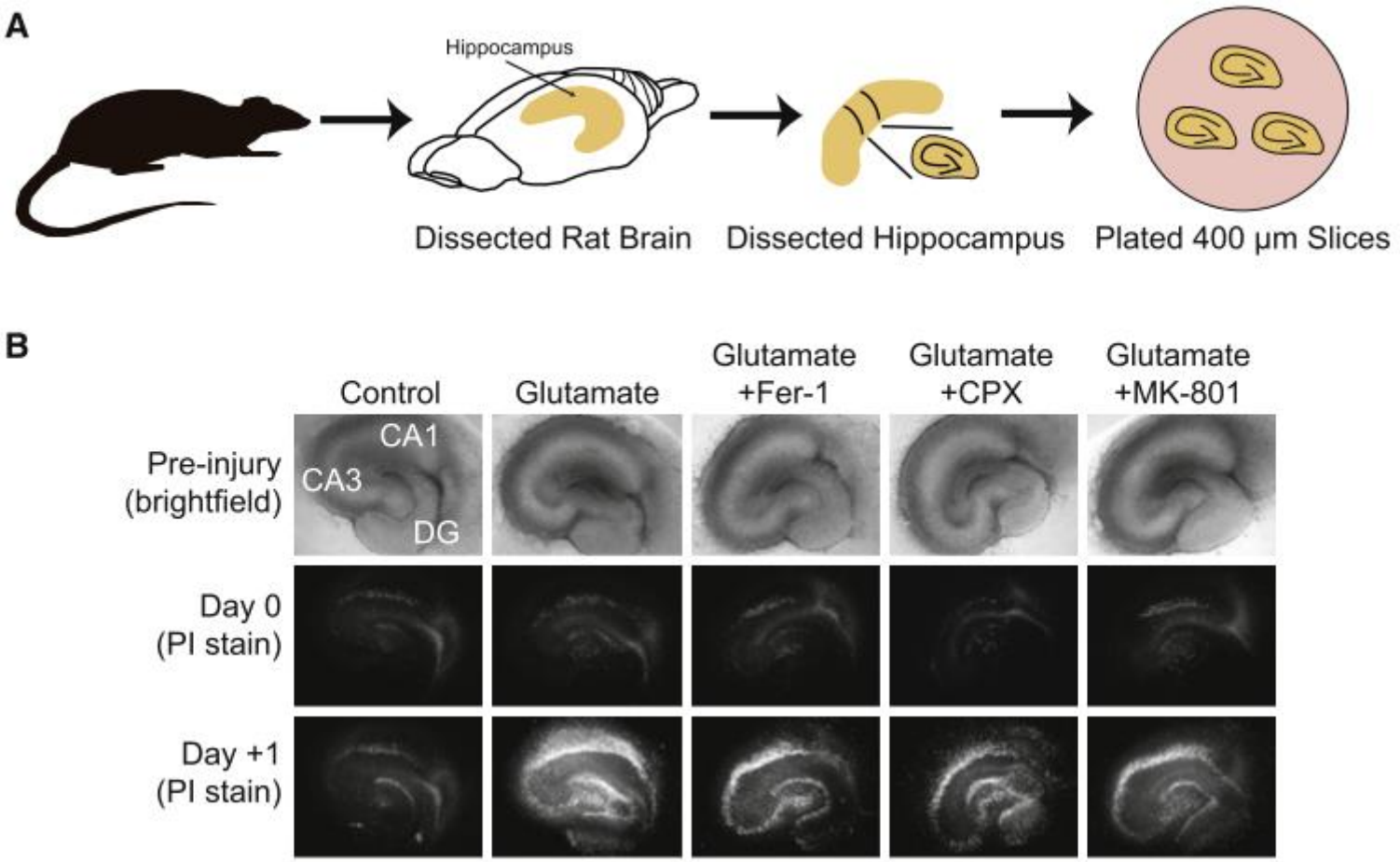

Dixon SJ, Lemberg KM, Lamprecht MR, et al (2012)
Ferroptosis: An iron-dependent form of nonapoptotic cell death.
Cell 149:1060–1072. doi: 10.1016/j.cell.2012.03.042

Ferroptózis – autofágia ?

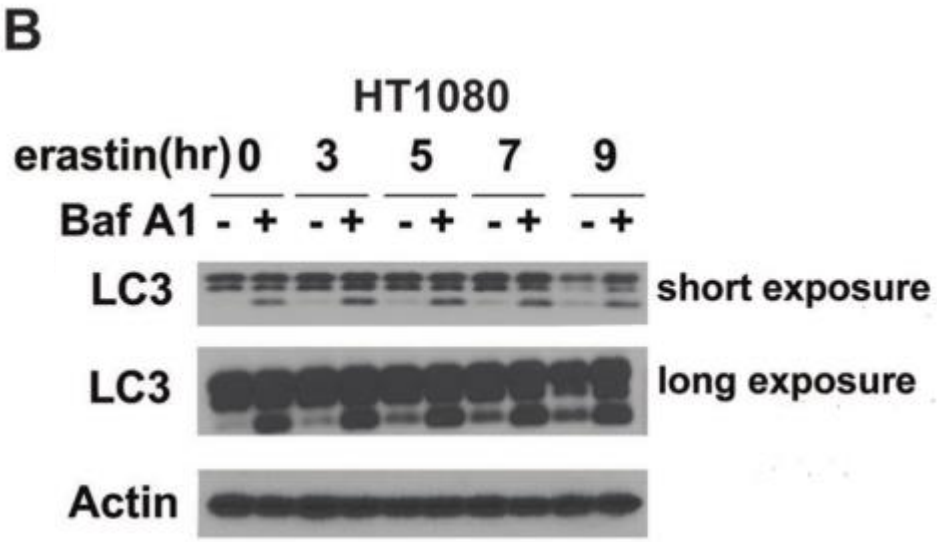

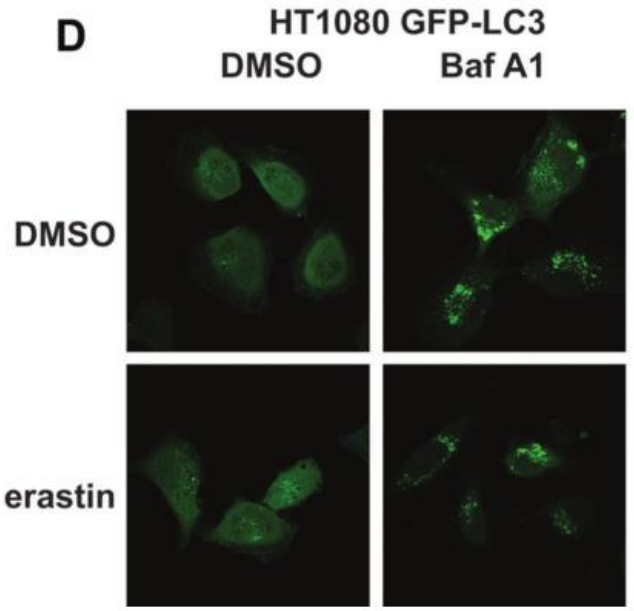

Gao M, Monian P, Pan Q, et al (2016)
Ferroptosis is an autophagic cell death process.
Cell Res 26:1021–32. doi: 10.1038/cr.2016.95

Autofágia mechaniumusa

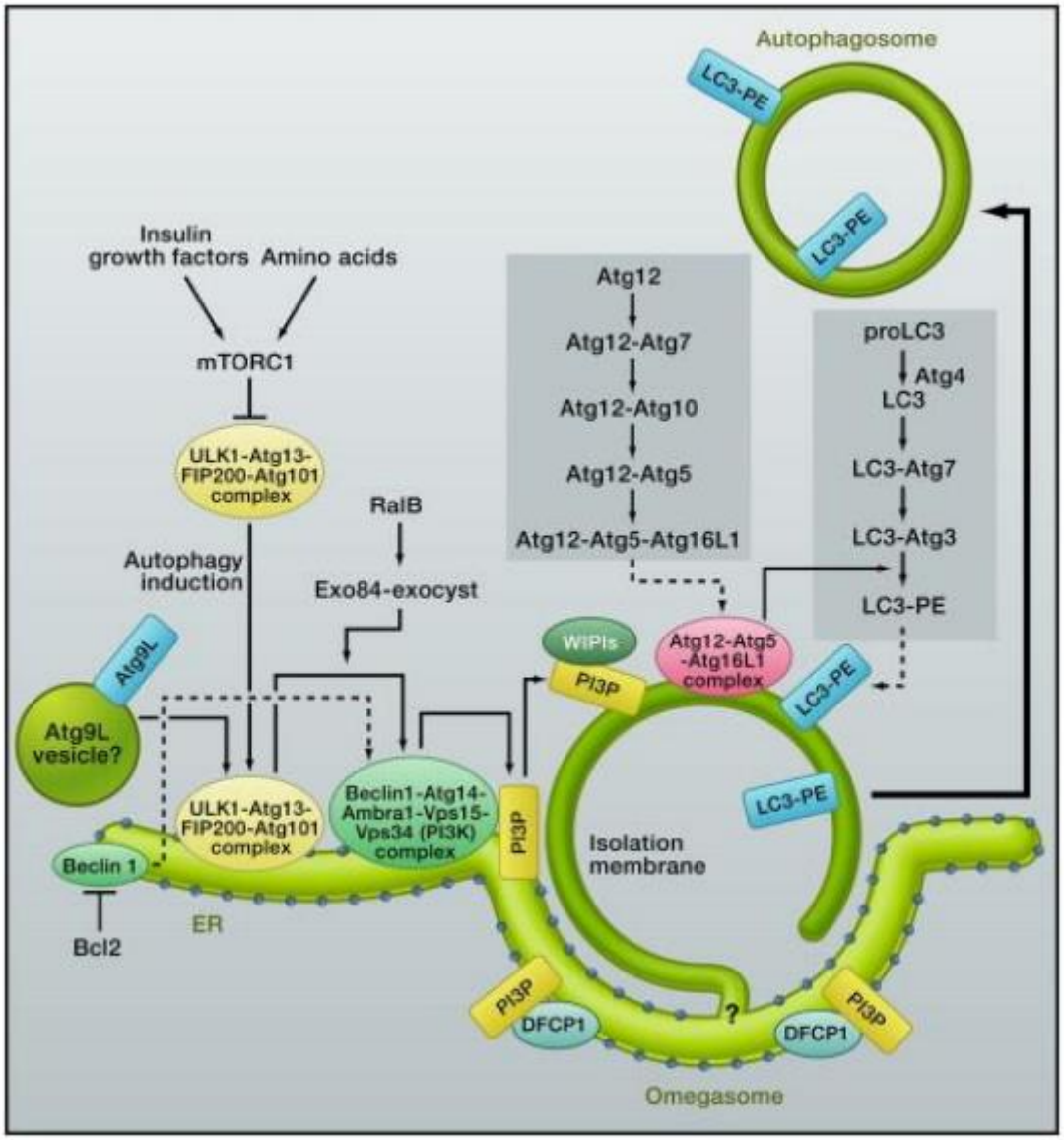

Ferroptózis – autofágia ?

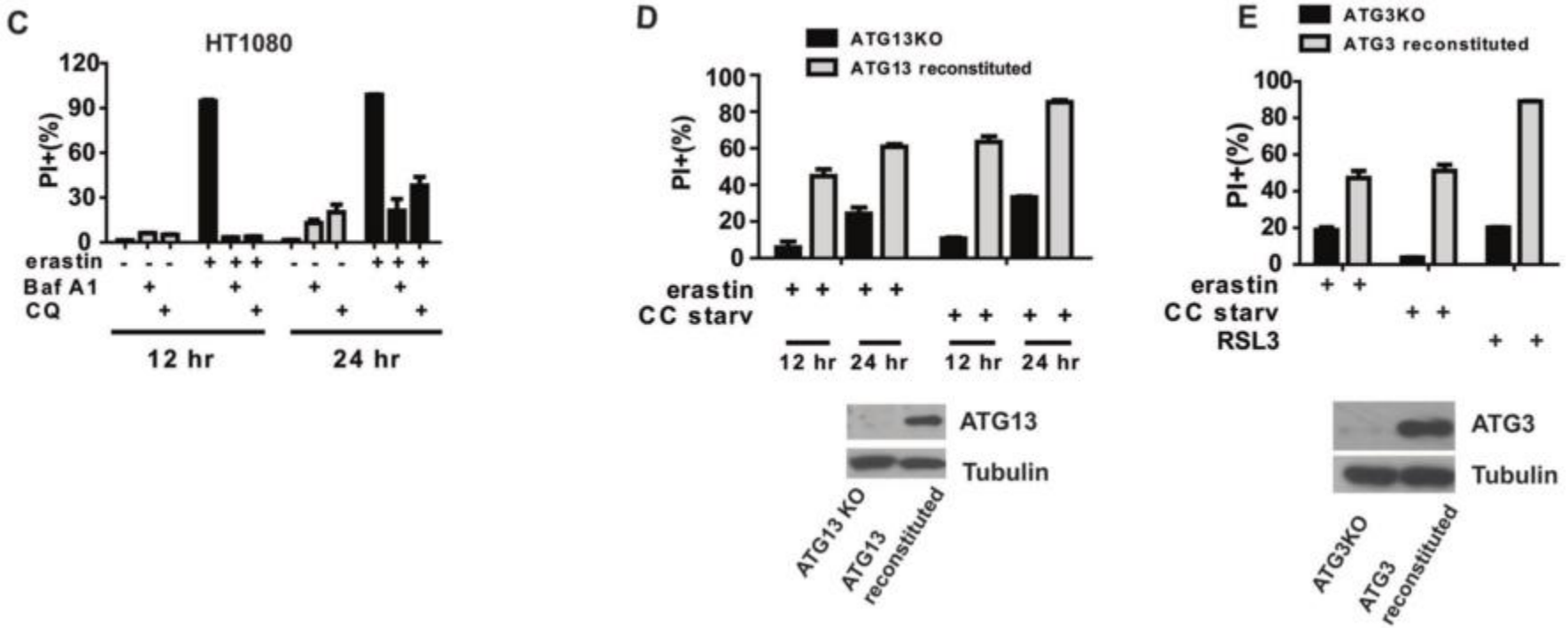

Gao M, Monian P, Pan Q, et al (2016)
Ferroptosis is an autophagic cell death process.
Cell Res 26:1021–32. doi: 10.1038/cr.2016.95

Ferroptózis – autofágia ?

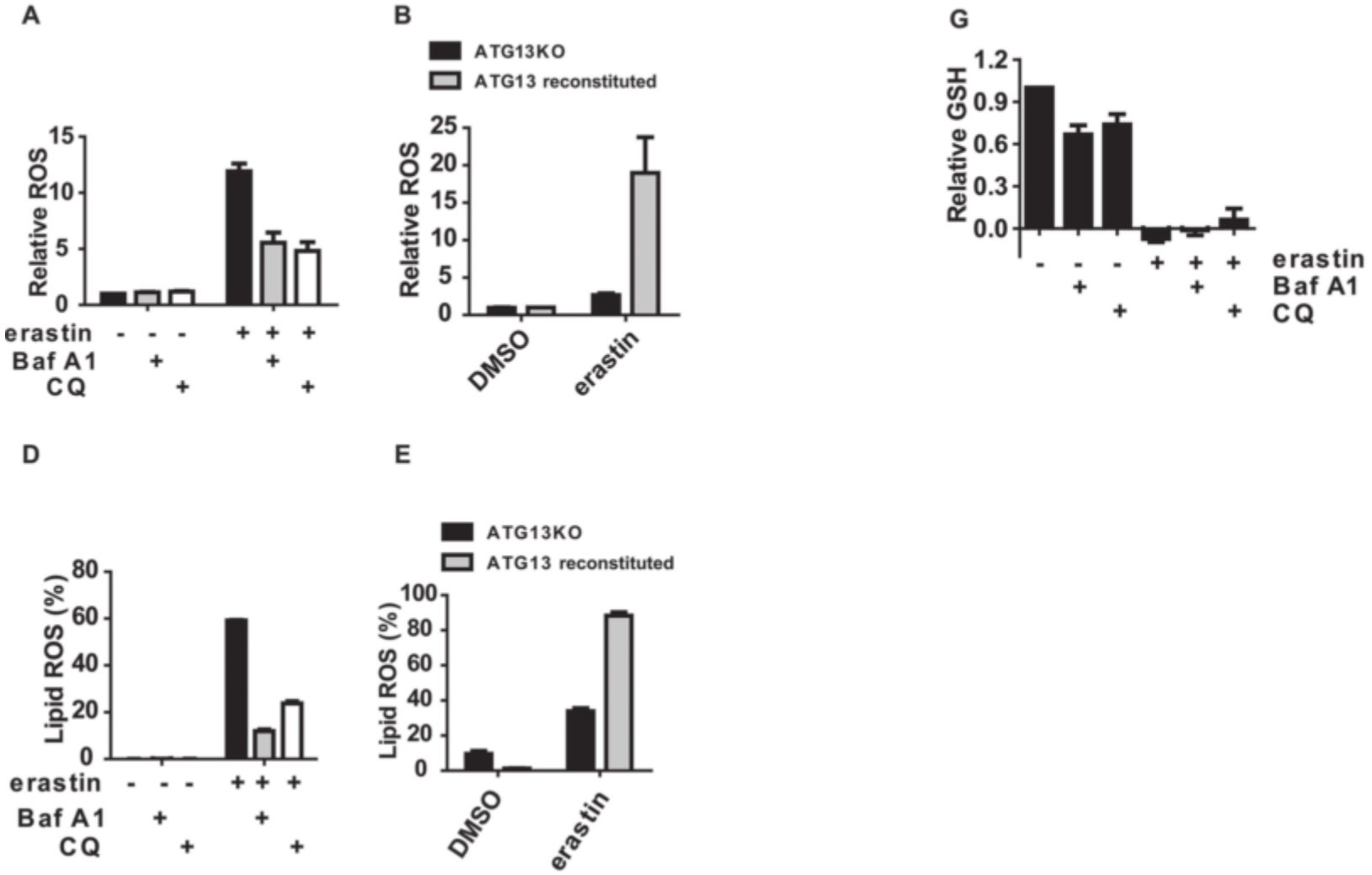

Gao M, Monian P, Pan Q, et al (2016)
Ferroptosis is an autophagic cell death process.
Cell Res 26:1021–32. doi: 10.1038/cr.2016.95

Ferroptózis – autofágia ?

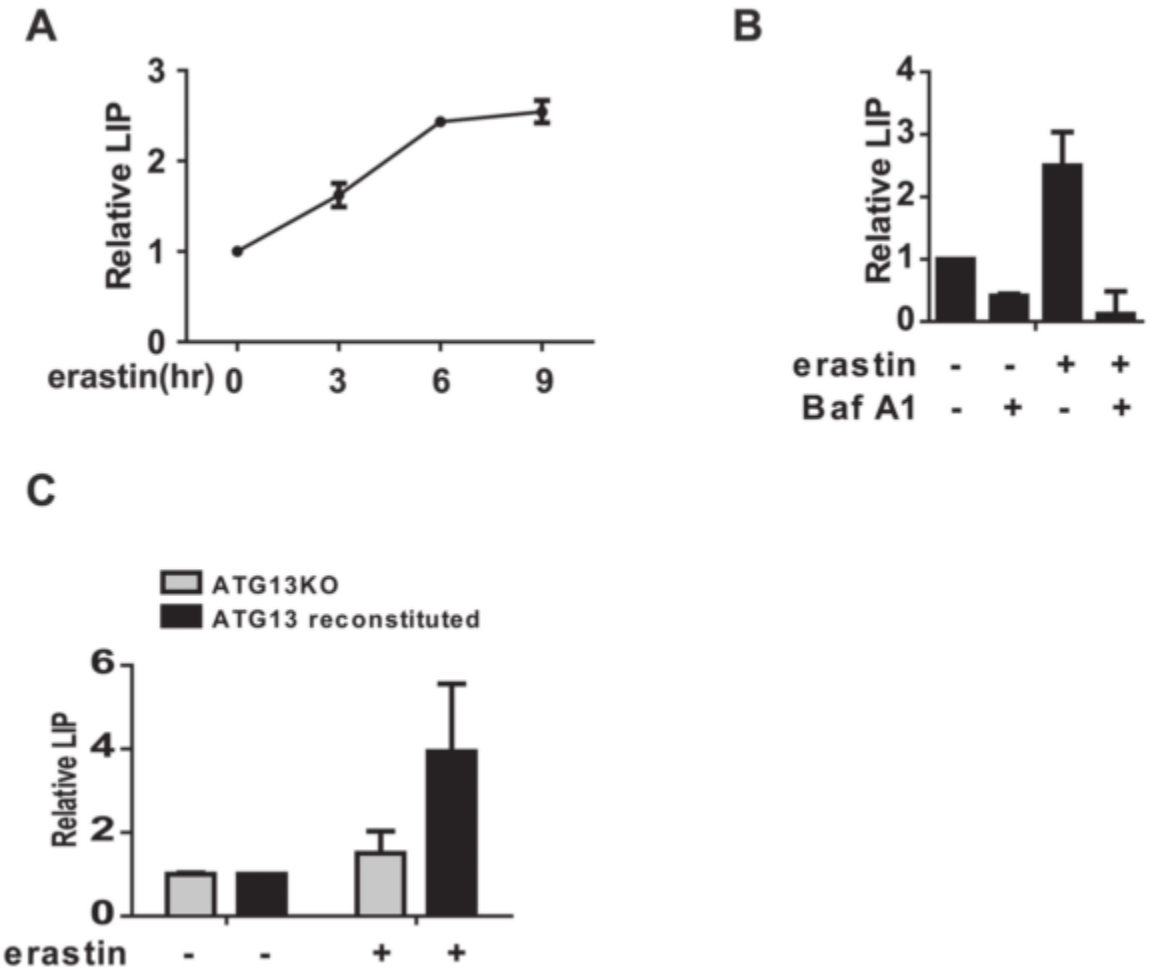

Gao M, Monian P, Pan Q, et al (2016)
Ferroptosis is an autophagic cell death process.
Cell Res 26:1021–32. doi: 10.1038/cr.2016.95

Ferroptózis (?)